

Magnetic behavior of a reentrant Ising spin glass

K. Gunnarsson, P. Svedlindh, J.-O. Andersson, P. Nordblad, and L. Lundgren
Department of Technology, Uppsala University, Box 534, S-751 21 Uppsala, Sweden

H. Aruga Katori and A. Ito

Department of Physics, Ochanomizu University, Bunkyo-ku, Tokyo 112, Japan

(Received 14 November 1991; revised manuscript received 27 April 1992)

The ac susceptibility of the reentrant Ising spin glass $\text{Fe}_{0.62}\text{Mn}_{0.38}\text{TiO}_3$ has been investigated in a superconducting-quantum-interference-device magnetometer. The data show a transition from a paramagnetic to an antiferromagnetic state at $T_N=32.8$ K. At lower temperatures, the in-phase component of the susceptibility, $\chi'(\omega)$, becomes frequency dependent and, simultaneously, a finite out-of-phase component of the susceptibility, $\chi''(\omega)$, appears. This behavior is interpreted to arise from a transition to a mixed spin-glass and antiferromagnetic state at $T_g=25.8$ K. A dynamic scaling analysis of $\chi''(\omega)$ yields critical exponents quite different from those found for the pure Ising spin glass $\text{Fe}_{0.5}\text{Mn}_{0.5}\text{TiO}_3$. However, some apparent deviations from optimal scaling behavior are observed. Magnetic relaxation experiments on this reentrant spin glass reveal the existence of an aging phenomenon similar to that observed in ordinary spin glasses. It is also found that the behavior of the magnetic relaxation can be interpreted within the context of spin-glass domain theories.

I. INTRODUCTION

The study of random magnets has been the focus of many physicists for several years.¹ Spin glasses, an intriguing class of disordered and frustrated magnetic systems, have been of special interest. Particular problems arise in systems where order and disorder coexist, as in *reentrant spin glasses* (RSG's). Most RSG's hitherto reported exhibit the coexistence of a ferromagnetic (FM) and a SG phase.² However, some compounds showing antiferromagnetic (AF) and SG order have been investigated, e.g., the Ising system $\text{Fe}_{0.55}\text{Mg}_{0.45}\text{Cl}_2$.³ Here, we present a study of the dynamic behavior and magnetic relaxation of the reentrant Ising spin glass $\text{Fe}_{0.62}\text{Mn}_{0.38}\text{TiO}_3$ using a superconducting-quantum-interference-device (SQUID) technique.

II. EXPERIMENTAL DETAILS

Magnetically, the system $\text{Fe}_x\text{Mn}_{1-x}\text{TiO}_3$ is well described by a hexagonal structure of honeycomb layers of Fe^{2+} or Mn^{2+} ions, where each magnetic ion is surrounded by three nearest neighbors. The system is Ising-like, with the magnetic moments directed along the hexagonal *c* axis. FeTiO_3 and MnTiO_3 are both antiferromagnets: In the former, there is FM order within the hexagonal layers and AF order between adjacent layers. The Fe^{2+} ion possesses strong single-ion anisotropy, yielding the Ising behavior.⁴ In the latter, there are both intra- and interlayer AF interactions and the anisotropy is caused by dipole-dipole interaction between the Mn^{2+} ions. When $0.38 < x < 0.58$, the random distribution of exchange interactions within the layers gives rise to a SG phase. $\text{Fe}_{0.5}\text{Mn}_{0.5}\text{TiO}_3$ is regarded as a model Ising spin glass, with a SG transition at $T_g \approx 20.7$ K. The dynamic and static magnetic behavior of this system has been ex-

tensively investigated.⁵⁻⁸ For $x \geq 0.58$ and $x \leq 0.38$, the system is antiferromagnetic, but also shows a reentrant AF-SG transition at concentrations just above $x=0.58$ and just below $x=0.38$. A complete phase diagram of the system $\text{Fe}_x\text{Mn}_{1-x}\text{TiO}_3$ is given in Ref. 4. Concerning $\text{Fe}_{0.62}\text{Mn}_{0.38}\text{TiO}_3$ (FMTO), the AF transition occurs at $T_N \approx 33$ K. At a lower temperature, T_g , the system enters a state with SG order.⁹

The sample, a single crystal of FMTO, was cut into the shape of a rectangular parallelepiped ($2 \times 2 \times 4$ mm) with the long axis parallel to the hexagonal *c* axis. The crystal was centered in one of the pickup coils of a third-order gradiometer, connected to a SQUID sensor. For the ac-susceptibility measurements, a magnetizing coil was wound directly onto the sample, yielding a small time-varying field, $h = h_0 \sin \omega t$ ($h_0 \approx 0.1$ G), parallel to the *c* axis. A second, similar coil was located in another part of the gradiometer to compensate for flux changes due to the direct influence from *h*. The ac susceptibility, $\chi(\omega) = \chi'(\omega) + i\chi''(\omega)$, was registered in the temperature interval $7 < T < 35$ K and in the frequency interval $5 \times 10^{-3} \leq \omega/2\pi \leq 5 \times 10^3$ Hz. An analog Princeton Applied Research model 5204 lock-in amplifier was used for $\omega/2\pi \geq 0.5$ Hz and a digital lock-in amplifier was used for $\omega/2\pi < 0.5$ Hz. The noise level ($\Delta\chi/\chi$) was 1×10^{-4} and 5×10^{-4} for the analog and digital lock-in amplifier, respectively. The zero-field-cooled (ZFC) magnetization measurements were performed as follows: In zero field, the sample was cooled from a temperature T_{ref} , well above T_g , to a temperature below T_g . After waiting a certain amount of time t_w at stable temperature, a small static field was applied parallel to the *c* axis and the relaxation of the ZFC magnetization, $M(t)$, was recorded. The measurements were performed at temperatures $11 \leq T \leq 27$ K and in the time interval $0.3 \leq t \leq 10\,000$ s. The magnitude of the field, typically $H=3$ G, is within the linear-response regime of $M(t)$ versus *H*.

III. RESULTS AND DISCUSSION

A. ac susceptibility

Figure 1 shows $\chi'(\omega)$ and $\chi''(\omega)$ versus temperature; the different curves correspond to different frequencies of the ac field. Studying Fig. 1(a), we observe a peak around $T = 34$ K, reflecting the AF transition: the maximum in $\partial\chi'T/\partial T$ versus T yields T_n (Ref. 10) (which here is located at 32.8 K). Furthermore, there is a frequency

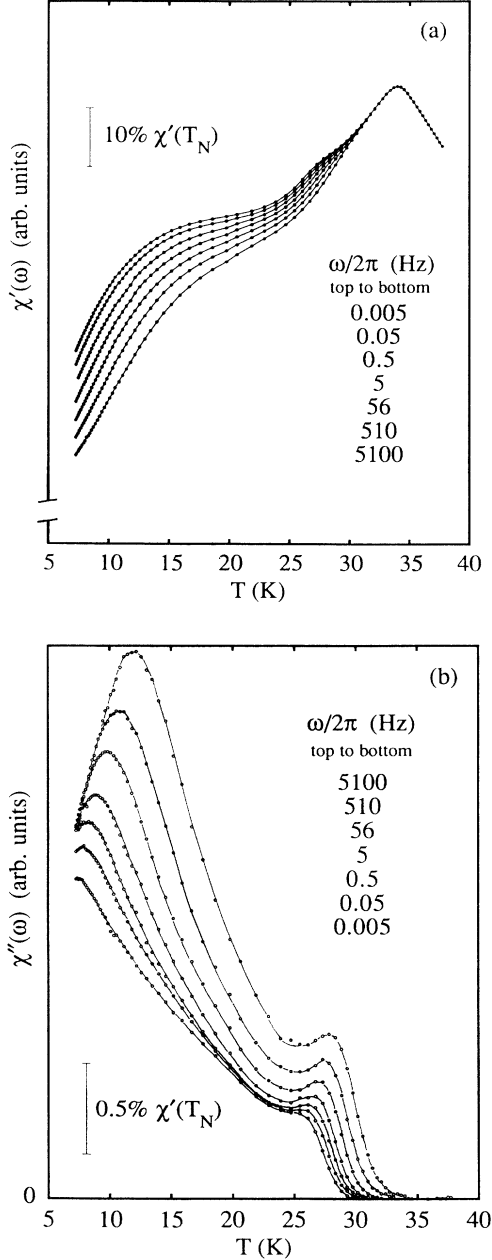


FIG. 1. $\chi'(\omega)$ and $\chi''(\omega)$ of the c axis ac susceptibility vs temperature. The different curves correspond to different frequencies of the applied ac field, $h_0 \approx 0.1$ G. $T_N = 32.8$ K and $T_g = 25.8$ K. (a) $\chi'(\omega)$ vs T . 10% of $\chi'(\omega)$ at T_N is indicated. (b) $\chi''(\omega)$ vs T . 0.5% of $\chi'(\omega)$ at T_N is indicated.

dependence of $\chi'(\omega)$ below ~ 30 K, a signature of SG behavior. This is also accompanied by the appearance of an out-of-phase component of the ac susceptibility, $\chi''(\omega)$, shown in Fig. 1(b). The $\chi''(\omega)$ curves exhibit *two maxima*, the first at $T \sim 30$ K and the second at $T \sim 10$ K.

In an ordinary SG system, e.g. $\text{Fe}_{0.5}\text{Mn}_{0.5}\text{TiO}_3$, the $\chi''(\omega)$ -versus- T curves are characterized by a rapid increase to a single maximum at $T > T_g$, followed by a continuous decrease to zero at $T = 0$.⁶ The initial behavior of $\chi''(\omega)$ versus T down to the first maximum [Fig. 1(b)] is quite similar to an ordinary spin-glass transition. The major difference compared to the transition in $\text{Fe}_{0.5}\text{Mn}_{0.5}\text{TiO}_3$ (Ref. 6) (and other three-dimensional spin glasses) being about a 4-times-lower value of the ratio $\chi''(\omega)/\chi'(\omega)$ at the first maximum in χ'' . The temperature and frequency dependence of χ'' can in this region be reasonably scaled according to classical dynamic scaling (and also activated dynamic scaling) as discussed below. However, on further decreasing the temperature, $\chi''(\omega)$ starts to increase and reaches a second maximum and finally decreases almost linearly towards zero at 0 K. This temperature dependence of $\chi''(\omega)$ is also reflected in an “S”-shaped character of $\chi'(\omega)$ on lowering the temperature towards zero. This peculiar dynamic behavior clearly distinguishes this spin-glass phase from an ordinary spin-glass phenomenon. A neutron-scattering investigation on the same compound by Yoshizawa *et al.*⁴ shows that the diffuse intensity increases below T_N , whereas the intensity of the antiferromagnetic Bragg peaks decreases. An interpretation of the ac susceptibility and the neutron data is that as the temperature is decreasing below T_N , an increasing number of spins leaves the antiferromagnetic order and enters a spin-glass “phase.” This also implies the coexistence of both an antiferromagnetic and a spin-glass phase at low temperatures.

The overall behavior of the susceptibility measured parallel to the c axis and the results from transverse susceptibility measurements primarily indicate the Ising character of the mixed spin-glass and antiferromagnetic behavior. Also, other susceptibility studies of $\text{Fe}_x\text{Mn}_{1-x}\text{TiO}_3$ on samples of other concentrations (x) show clear Ising properties. However, results from Mössbauer-spectroscopy studies on this sample^{11,12} and on $\text{Fe}_{0.5}\text{Mn}_{0.5}\text{TiO}_3$ (Ref. 13) have been interpreted to show a large canting of the Fe spins (an angle of 45° and 60° relative to the c axis, respectively). This result is quite puzzling and almost paradoxical when combined with the susceptibility behavior.

B. Dynamic scaling

The spin-glass relaxation occurs over a time window that is narrow at high temperatures and broadens with decreasing temperature. Assuming critical slowing down on approaching T_g from above, the maximum relaxation time τ_{max} follows:¹⁴

$$\tau_{\text{max}} = \tau_0 (T_f/T_g - 1)^{-z\nu}, \quad (1)$$

where τ_0 is the single-spin-flip time ($\approx 10^{-13}$ s) and $z\nu$ is a dynamic exponent. If T_f is identified as the tempera-

ture where $\chi'(\omega)$ deviates from the equilibrium (static) value, $\tau_{\max}(T_f) = \omega^{-1}$. This temperature coincides with the inflection-point temperature of $\chi''(\omega)$ versus T . Using this definition of T_f , the best fit of the data in Fig. 1(b) to Eq. (1) yields $z\nu = 13 \pm 2$ for $T_g = 25.8 \pm 0.4$ K. Geschwind *et al.*¹⁵ have proposed the following dynamic scaling equation to be valid for SG systems:

$$\chi''T/\omega^{\beta/z\nu} = f(\varepsilon/\omega^{1/z\nu}), \quad (2)$$

where $\varepsilon = T/T_g - 1$, β is a critical exponent, and $f(x = \varepsilon/\omega^{1/z\nu})$ is a scaling function; $f(x) \rightarrow \text{const}$ when $x \rightarrow 0$. Using a correct set of parameters, all $\chi''(\omega)$ -versus- T curves should collapse onto the same curve in a scaling plot according to Eq. (2). The maximum, χ''_{\max} , of each curve in Fig. 1(b) will be imaged to the same point in the scaling plot. Utilizing this property, Eq. (2) can be simplified:

$$\chi''_{\max} T (\chi''_{\max}) \propto \omega^{\beta/z\nu}. \quad (3)$$

This equation provides a method of both estimating $\beta/z\nu$ separately and of reducing the number of free parameters in Eq. (2). Using the data in Fig. 1(b), the best fit to Eq. (3) was obtained for $\beta/z\nu = 0.071 \pm 0.005$. Guided by the results above, we now perform a complete scaling plot according to Eq. (2). Figure 2 displays $\chi''T/\omega^{\beta/z\nu}$ versus $\varepsilon/\omega^{1/z\nu}$, where $\beta/z\nu = 0.071$, $T_g = 25.8$ K, and $z\nu = 13$, which yields the best data collapse. Thus, the value of β will be 0.9 ± 0.1 . The values of the critical exponents can be compared to $z\nu = 10$ and $\beta = 0.54$ reported for $\text{Fe}_{0.5}\text{Mn}_{0.5}\text{TiO}_3$.^{6,8} The quality of this data collapse is not perfect; some deviations from satisfactory scaling are always observed in the analysis. One explanation for the deviations can be the comparatively low magnitude of χ'' in the scaling region. Another possible reason for non-perfect collapse is the influence of *aging*, i.e., the nonequilibrium character of χ'' measured in the vicinity of (and below) T_g .^{16,17} However, we have accounted for that problem by omitting all data that could be affected by aging. The main reason for the deviations from satisfactory scaling behavior is, instead, the increasing number of spins contributing to the spin-glass phase as the temperature is lowered (cf. the discussion above). This

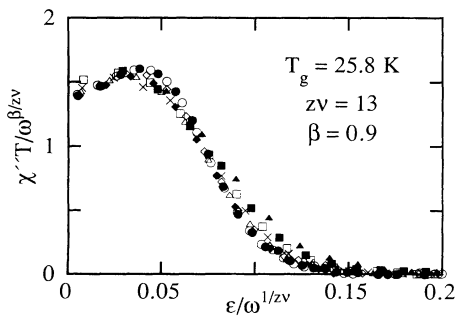


FIG. 2. $\chi''T/\omega^{\beta/z\nu}$ vs $\varepsilon/\omega^{1/z\nu}$ where $\varepsilon = T/T_g - 1$ and the parameters have the following values: $T_g = 25.8$ K, $z\nu = 13$, and $\beta/z\nu = 0.071$. The following frequencies have been used, $\omega/2\pi$ (Hz): 0.5 (\blacktriangle), 1.7 (\blacksquare), 5 (\square), 17 (\times), 56 (\triangle), 170 (\blacklozenge), 510 (\diamond), 1700 (\bullet), and 5100 (\circ).

property of our system obscures the analysis and may also result in effective values of the critical exponents that are different from their true Ising values. To our knowledge, no dynamic scaling analysis of an AF-to-AF-SG transition has been reported previously. A dynamic scaling analysis of preliminary data on this system was reported by us in Ref. 18.

The high value of $z\nu$ obtained in the conventional dynamic scaling analysis may indicate that activated dynamic scaling, originally proposed for random-field (RF) Ising systems, should be the appropriate scaling approach in FMTO. However, such an analysis also shows deviations from satisfactory scaling behavior similar to those illustrated in the classical analysis described above.

C. Aging

An ordinary spin glass is subject to an aging process at time scales shorter than the maximum relaxation time in the system. After a temperature quench from a high-temperature, T_{ref} , to a lower temperature, T , the SG system only approaches equilibrium logarithmically slow. This nonequilibrium property can be observed in ZFC magnetization experiments, where the response will vary with the wait time at constant temperature prior to the field application, i.e., $M(t) = M(t_w, t)$.

In order to reveal a possible aging behavior of FMTO in the AF-SG phase, ZFC magnetization experiments have been performed. Figure 3 shows the relaxation rate, $S(t) = \partial M(t)/\partial \ln t$, versus $\log_{10}(t)$ for three different values of t_w at $T/T_g = 0.75$. All these curves display pronounced maxima at $\log_{10}(t) \approx \log_{10}(t_w)$, the very signature of the aging process in ordinary spin glasses.¹⁹ In plots of $M(t)$ versus $\log_{10}(t)$ these maxima appear as clear inflection points at $\log_{10}(t) \approx \log_{10}(t_w)$. Figure 3 confirms that the reentrant AF-SG phase of FMTO is subject to an aging process similar to that of an ordinary spin glass, which also implies (as has been evidenced from extensive studies on different spin-glass systems²⁰) that

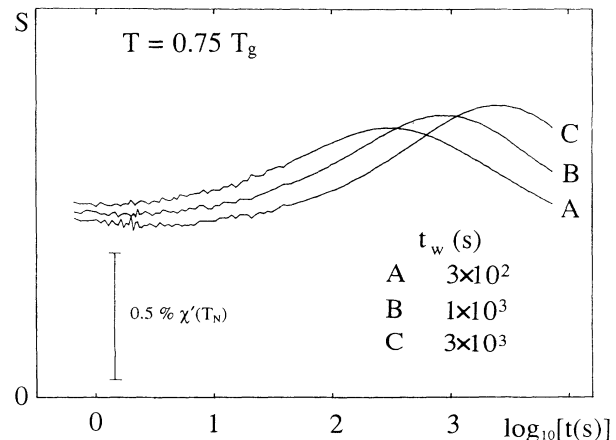


FIG. 3. $S = \partial M / \partial \log_{10}(t)$ vs $\log_{10}(t)$ at $T = 0.75 T_g$ ($T_g = 25.8$ K). The different curves correspond to different wait times t_w at T prior to the application of $H = 1$ G. 0.5% of $\chi'(\omega)$ at T_N is indicated.

$M(t)$ probes equilibrium dynamics at time scales of $\log_{10}(t) \ll \log_{10}(t_w)$. A specific study of the influence of aging on the measured ac susceptibility has been performed on $\text{Fe}_{0.5}\text{Mn}_{0.5}\text{TiO}_3$.¹⁷ Analysis of these data shows that aging results in a nonequilibrium character of $\chi''(\omega)$ and that the measured value of $\chi''(\omega)$ slowly evolves with time (until the system is kept at a constant temperature for a time $t \approx 1/\omega \approx \tau_{\text{max}}$). The equivalence in the dynamic properties between FMTO and ordinary spin-glass systems implies that the low-frequency ac-susceptibility data close to T_g are affected by nonequilibrium influences and must be omitted in the dynamic scaling analysis.

D. Spin-glass domains

Referring to SG domain theory,^{21,22} the characteristics of Fig. 3 can be interpreted as follows: At T there is a growth of SG domains containing the equilibrium spin correlations $\{s_i\}$. The domains are characterized by a length $R \sim [T \ln(t + t_w)/\Delta]^{1/\Psi}$ (Ψ is the barrier-height exponent). $M(t)$ probes relaxation processes on a “length scale” L , which grows in a way similar to R after the application of H , i.e., $L \sim [T \ln(t)/\Delta]^{1/\Psi}$. As long as $L \ll R$, equilibrium dynamics will be measured. When $\ln(t) \approx \ln(t_w)$, $L \sim R$ and there is a crossover to nonequilibrium dynamics, which is reflected by the maximum of $S(t)$ versus $\log_{10}t$ at $\log_{10}(t) \approx \log_{10}(t_w)$.

In identifying a SG system, aging is a necessary but insufficient feature. It may also be found in other disordered systems.¹ However, in the SG $\{s_i\}$ is unique for each temperature, and at two temperatures T and $T + \Delta T$, there is an overlap of $\{s_i\}$ only up to a certain overlap length scale, $l_{\Delta T}$. Hence, if we perform a ZFC experiment, and after t_w , prior to the field application, make a short temperature cycling ΔT , $S(t)$ will show either of the following behaviors: (1) ΔT is small, $l_{\Delta T} > R$, and there will be no major difference in $S(t)$ as compared to $\Delta T = 0$. (2) ΔT is sufficiently large, $l_{\Delta T} < R$, the “old” domains will start to break up, and “young” domains will start to grow from $l_{\Delta T}$; hence, the $S(t)$ -versus- $\log_{10}(t)$ curve will exhibit two maxima, due to the two characteristic domain sizes²³ (the position of the first maximum, corresponding to the “young” domains, is largely due to the experimental cooling rate). (3) ΔT is large, the “old” domains are destroyed, and $S(t)$ reflects the effect of “young” domains only.

Figure 4 shows $S(t)$ versus $\log_{10}(t)$ from such a ZFC experiment, with $T = 0.75T_g$ and $t_w = 10^4$ s. ΔT was varied in the interval $0 \leq \Delta T \leq 4.6$ K, yielding the different curves shown in the figure. Also, an “infinite” step is included, i.e., a step such that $T + \Delta T > T_g$. Indeed, $S(t)$ display the behaviors outlined above. For $\Delta T \leq 0.65$ K, $S(t)$ remains quite unaffected, i.e., a maximum occurs at $\log_{10}(t) \approx \log_{10}(t_w = 10^4 \text{ s})$. The growth

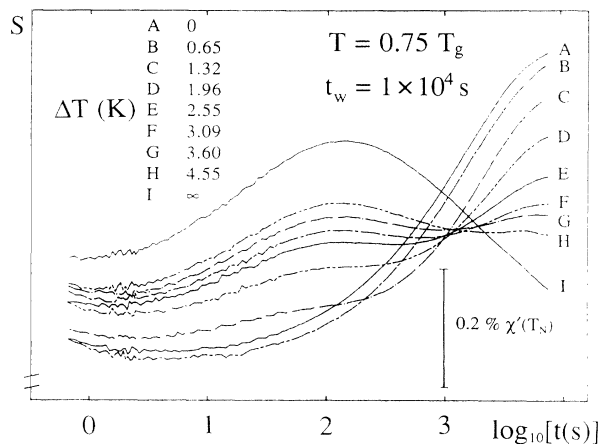


FIG. 4. $S = \partial M / \partial \log_{10}(t)$ vs $\log_{10}(t)$ at $T = 0.75T_g$ ($T_g = 25.8$ K), $H = 3$ G. The different curves correspond to different temperature pulses, applied after $t_w = 10^4$ s. 0.2% of $\chi'(\omega)$ at T_N is indicated.

rate of the domains is increased during the cycling to $T + \Delta T$. Therefore, the system appears to be somewhat older after the cycling. For $0.65 < \Delta T < 4.6$ K, the curves mirror the “old” domains of size $R(t_w = 10^4 \text{ s})$ and the “young” domains. Here, two maxima are observed. Finally, for the “infinite” step, the curve is similar to the result of an ordinary ZFC experiment with $t_w = 0$.

IV. SUMMARY

ac-susceptibility measurements on the reentrant spin-glass system $\text{Fe}_{0.62}\text{Mn}_{0.38}\text{TiO}_3$ reveal an extraordinary behavior of $\chi''(\omega)$ below T_g . A dynamic scaling analysis of ac-susceptibility data at the transition from an AF phase to an AF-SG phase is performed. The critical exponents extracted are $z\nu = 13$ and $\beta = 0.9$. These values are different from those reported on the Ising SG $\text{Fe}_{0.5}\text{Mn}_{0.5}\text{TiO}_3$.^{6,8} However, due to the very different dynamics of FMTO at low temperatures compared to an ordinary spin glass, it is possible that these differences only reflect that effective values of the critical exponents, different from the true Ising values, are obtained from the scaling analysis. Below T_g , FMTO shows characteristic properties of a true spin-glass phase, e.g., aging. Also, the response to temperature-cycling experiments is similar to that of ordinary spin glasses. These results are also interpreted to support the validity of droplet theories for the spin-glass phase.

ACKNOWLEDGMENT

Financial support from the Swedish Natural Science Research Council (NFR) is acknowledged.

- ¹D. Fisher, G. Grinstein, and A. Khurana, *Phys. Today* **41**(12), 56 (1988).
- ²See, e.g., T. Satoh, *J. Phys. Soc. Jpn.* **57**, 1743 (1988); Ph. Mangin, D. Boumazouza, B. George, J. Rhyne, and R. Erwin, *Phys. Rev. B* **40**, 11 123 (1989).
- ³P. Wong, S. v. Molnar, T. Palstra, J. Mydosh, H. Yoshizawa, S. M. Shapiro, and A. Ito, *Phys. Rev. Lett.* **55**, 2043 (1985).
- ⁴H. Yoshizawa, S. Mitsuda, H. Aruga, and A. Ito, *J. Phys. Soc. Jpn.* **58**, 1416 (1988).
- ⁵A. Ito, H. Aruga, E. Torikai, M. Kikuchi, Y. Syono, and H. Takei, *Phys. Rev. Lett.* **57**, 483 (1986).
- ⁶K. Gunnarsson, P. Svedlindh, P. Nordblad, L. Lundgren, H. Aruga, and A. Ito, *Phys. Rev. Lett.* **61**, 754 (1988).
- ⁷P. Svedlindh, K. Gunnarsson, P. Nordblad, L. Lundgren, H. Aruga, and A. Ito, *Phys. Rev. B* **40**, 7162 (1989).
- ⁸K. Gunnarsson, P. Svedlindh, P. Nordblad, L. Lundgren, H. Aruga, and A. Ito, *Phys. Rev. B* **43**, 8199 (1991).
- ⁹H. Aruga, A. Ito, H. Wakabayashi, and T. Goto, *J. Phys. Soc. Jpn.* **57**, 2636 (1988).
- ¹⁰M. E. Fisher, *Philos. Mag.* **7**, 1731 (1962).
- ¹¹A. Seidel, K. Gunnarsson, P. Svedlindh, L. Häggström, H. Aruga Katori, and A. Ito, *J. Magn. Magn. Mater.* **104-107**, 1599 (1992).
- ¹²The Mössbauer spectra for $T < T_n$ are broad patterns, characteristic of disordered materials, and each spectrum is treated as a superposition of two different subspectra due to "paramagnetic" (the relaxation time of the spins is shorter than the characteristic time of the Mössbauer experiment, $\sim 10^{-7}$ s) and canted spins. Upon reducing the temperature towards T_g , the relative intensity of the canted subspectrum grows at the expense of the "paramagnetic" subspectrum. The mean canting angle θ is $\sim 45^\circ$.
- ¹³A. Ito, E. Torikai, S. Morimoto, H. Aruga, M. Kikuchi, Y. Syono, and H. Takei, *J. Phys. Soc. Jpn.* **59**, 829 (1990).
- ¹⁴P. Hohenberg and B. Halperin, *Rev. Mod. Phys.* **49**, 435 (1977).
- ¹⁵S. Geschwind, D. Huse, and G. Devlin, *Phys. Rev. B* **41**, 4854 (1990).
- ¹⁶L. Lundgren, P. Svedlindh, and O. Beckman, *J. Magn. Magn. Mater.* **31-34**, 1349 (1983).
- ¹⁷P. Svedlindh, K. Gunnarsson, J.-O. Andersson, H. Aruga Katori, and A. Ito, *Phys. Rev. B* (to be published).
- ¹⁸J.-O. Andersson, K. Gunnarsson, P. Svedlindh, P. Nordblad, L. Lundgren, H. Aruga, and A. Ito, *Physica B* **165&166**, 183 (1990).
- ¹⁹L. Lundgren, P. Nordblad, P. Svedlindh, and O. Beckman, *J. Appl. Phys.* **57**, 3371 (1985).
- ²⁰P. Granberg, P. Svedlindh, P. Nordblad, and L. Lundgren, in *Experiments on Relaxation in Metallic Spin Glasses*, Proceedings of the Heidelberg Colloquium on Glassy Dynamics, edited by J. L. van Hemmen and I. Morgenstern (Springer, Heidelberg, 1987); P. Svedlindh, K. Gunnarsson, P. Nordblad, L. Lundgren, H. Aruga, and A. Ito, *J. Magn. Magn. Mater.* **71**, 22 (1987).
- ²¹G. Koper and H. Hilhorst, *J. Phys. (France)* **49**, 429 (1988).
- ²²D. Fisher and D. Huse, *Phys. Rev. B* **38**, 373 (1988).
- ²³L. Sandlund, P. Svedlindh, P. Granberg, P. Nordblad, and L. Lundgren, *J. Appl. Phys.* **64**, 5616 (1988).